Available online at www.sciencedirect.com
SCIENCE DIRECT
Polymer 46 (2005) 6706–6714
polymer
www.elsevier.com/locate/polymer

Poly(ethylene terephthalate) ionomer based clay nanocomposites produced via melt extrusion

Grant D. Barber, Bret H. Calhoun, Robert B. Moore*

School of Polymers and High Performance Materials, The University of Southern Mississippi, 118 College Drive #10076, Hattiesburg, MS 39406-0001, USA

Available online 13 June 2005

Abstract

Poly(ethylene terephthalate) ionomer (PETI)/organically-modified montmorillonite clay (OMC) nanocomposites were prepared via melt extrusion. Sulfonated PET containing various incorporations of ionic comonomer and clay modifications were investigated. The random incorporation of ionic functionalities along the PET backbone enhances interactions between the matrix polymer and montmorillonite clay resulting in the creation of polymer-clay nanocomposites exhibiting a predominately exfoliated morphology. The morphology is correlated with mechanical properties and crystallization behavior. It is found that incorporation of clay into the random ionomers leads to increased mechanical properties and slower crystallization rates.

Keywords: PET nanocomposites; Ionomeric compatibilizer; Morphology

1. Introduction

Nanocomposites refer to solid, multiphase materials in which at least one dimension of a dispersed phase is in the nanometer range, typically 1–20 nm. Polymeric, intercalation-type nanocomposites have been the subject of extensive research in both academia and industry over the past decade [1–4]. One of the challenges in producing polymer/clay nanocomposites with enhanced properties is tailoring the morphology (i.e. intercalated or exfoliated) of the system and the interaction of the polymer matrix with the inorganic particles.

Considering the improvements in reduced gas permeability and enhanced mechanical properties [5–8] that are commonly observed with the addition of clay into polymers, investigations of PET based clay nanocomposites have previously been made. Many experimental studies have relied on the in situ creation of the PET nanocomposite to develop an intercalated or exfoliated morphology [9–12]. In the in situ method of creating nanocomposites, monomer and nanoscopic filler are dispersed and polymerization is carried out. The chain growth in or around the particles promotes nanocomposite formation having intercalated or exfoliated morphologies. Ke and coworkers have examined the crystallization process and crystal morphology of PET-clay nanocomposites prepared via in situ methods and have shown that clay content affects the crystallinity and takes on the role of a nucleating reagent [13]. The researchers also suggested that the distribution of intercalated aggregates and exfoliated clay platelets also plays an important role in the crystallization of PET. At high montmorillonite (MMT) concentrations, i.e. greater than 3 wt%, the crystallization of the PET was hindered. The decrease in the crystallization was attributed to the increased interactions with the large number of clay platelets present. Examples of intercalated, exfoliated and agglomerated (tactoid) morphologies were seen depending on the amount of organically modified clay added to the initial reaction mixture. The dispersion of the clay platelets was also observed to be controlled by surface modification and the polymerization procedures [14].

Many researchers have attempted to facilitate better dispersion of nanofillers in PET nanocomposites by utilizing novel compatibilizers [15–17]. Imai and coworkers found that the addition of a compatibilizer, 10-[3,5-bis(methoxycarbonyl)phenoxy]decyltriphenylphosphonium bromide (IP10TP), to a PET/mica nanocomposite prepared via a two-step polymerization procedure led to better dispersion of the mica [18]. However, X-ray diffraction studies clearly show a layered ordering still present in the nanocomposites (an intercalated morphology). The resulting nanocomposite

* Corresponding author. Tel.: +1 601 266 4480; fax: +1 601 266 5504.
E-mail address: rbmoore@usm.edu (R.B. Moore).

0032-3861/$ - see front matter © 2005 Elsevier Ltd. All rights reserved.
doi:10.1016/j.polymer.2005.05.024

also exhibited higher tensile properties when compared to a PET/mica nanocomposite prepared with no compatibilizer. Sanchez-Solis and coworkers reported PET–montmorillonite (MMT) clay nanocomposites utilizing compatibilizers prepared via an extrusion process [19]. Pentaerythrytol and maleic anhydride were used as additives in the extrusion process to attempt to compatibilize the PET with an organically modified MMT (Cloisite® 15A). The morphology of the system was investigated by XRD, and it was concluded that the system investigated did not display an exfoliated morphology. With large incorporations of the compatibilizers and increasing clay concentrations, an increase in the percent crystallinity was observed for the extruded pellets. This behavior was attributed to the large clay aggregates acting as a nucleating agent.

A melt or extrusion process is a more industrially viable route to the creation of nanocomposite materials. Davis et al. examined two systems prepared via twin-screw extrusion utilizing different organic modifiers [20]. One system utilizing a commercial alkyl ammonium modifier, *N*,*N*-dimethyl-*N*,*N*-dioctadecylammonium, created black, brittle nanocomposites resulting from modifier degredation. The second system utilized 1,2-dimethyl-3-*N*-hexadecyl imidazolium tetrafluoroborate exhibited high levels of dispersion in TEM. Pegoretti [21] has examined nanocomposites of recycled PET (rPET) with sodium form MMT (Cloisite® Na+) and an organically modified MMT (Cloisite® 25A) prepared through melt compounding and injection molding. Transmission electron microscopy (TEM) clearly showed that the organically modified Cloisite® 25A is much better dispersed in the rPET matrix. However, the TEM combined with XRD results demonstrated that while the lamellar periodicity d_{001} of the clay was increased, the morphology remained intercalated. It was also found that the Cloisite® 25A exhibited a larger tensile modulus relative to the Cloisite® Na+. This effect was attributed to the better dispersion of clay in the rPET matrix.

The role that nanoparticles play in the crystallization behavior of PET nanocomposites has been reported in the literature [22,23]. Ou et al. [24,25] have found that for solution prepared nanocomposites, clay lowered the half-time of crystallization and is an effective nucleating agent when an intercalated morphology developed. Other research has shown that the incorporation of organically modified montmorillonite clays, such as Cloisite® 30A, via solution blending have significantly increased the crystallization temperature while lowering the crystallization half-time [26]. In this study, Barber found that exfoliated nanoparticles with bound ionomer are less effective nucleants relative to the large clay aggregates. Other studies have shown that ionomeric content alone also affects the overall crystallinity of PET [26–28].

Because of the charged nature of the aluminosilicate surfaces of montmorillonite clay, our interests are to determine the effect ionic groups present in a semicrystalline polymer have on the morphology of montmorillonite composites. In previous work [29], we have investigated the effect of ionic incorporation on the morphology and crystallization of poly(butylene terephthalate) (PBT) and PBT containing random ionic functionalities along the backbone. The incorporation of as little as 1 mol% of ionic content was found to significantly affect the morphology and achieve considerable exfolitation of the nanocomposites. The degree of exfoliation was not found to be strongly dependant upon the amount of ionic incorporation. However, the mechanical properties were seen to increase as the ionic content was raised. This was attributed to the increased interactions between the polymer matrix and the clay platelets.

The semicrystalline, ion-containing polymer chosen for this investigation was sulfonated poly(ethylene terephthalate). Organically modified montmorillonite clays and sodium montmorillonite will be introduced into the pure PET and PET ionomers through a melt extrusion process and compared to determine the influence of the ionic functionality on clay platelet dispersion in addition to the effect on the crystallization behavior.

2. Experimental

2.1. Materials

The poly(ethylene terephthalate) (PET), Eastapak® 7352, was obtained from Eastman Chemical Company. PET-ionomers, shown in Fig. 1, were also received from Eastman Chemical Company containing ionic contents of 1.8, 3.9 and 5.8 mol% and will be abbreviated as PETI(1.8%), PETI(3.9%) and PETI(5.8%), respectively. Sodium montmorillonite (Cloisite® Na+) and the organically modified montmorillonite (Cloisite® 10A and Cloisite® 15A) were obtained from Southern Clay Products. All polymer materials were dried to below 0.02% moisture content and the organically modified montmorillonite was dried under vacuum for 12 h at 100 °C prior to melt processing. All materials were used without further purification with formulations based on dry mass.

2.2. Material processing

The materials were compounded using a Prism 16 mm twin screw extruder (25:1 *L*/*D*). The temperature profile (throat to die) was as follows: 240, 255, 255, 255 and 240 °C with a screw speed of 400 rpm. A dry nitrogen flow was supplied to both the hopper and the feeder to aid in maintaining dry materials. The clay and polymer were dry mixed prior to being fed into the hopper. The resulting nanocomposite strand was cooled in a water bath, pelletized and dried overnight in vacuum at 60 °C. ASTM D-638 type I dumbbell shaped specimens were molded using a Boy 15S injection molding machine. The barrel temperature was set to 260 and 265 °C and an injection speed of 2.5 in./s was

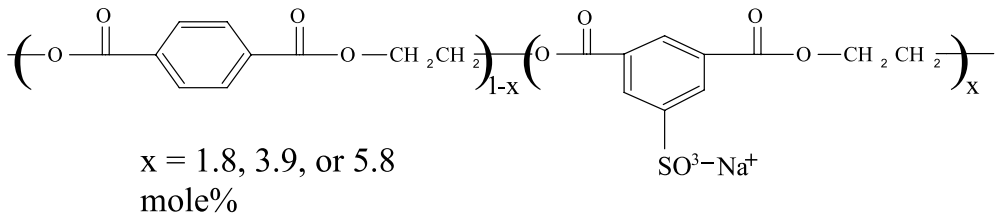

Fig. 1. Structure of PET and PETI polymers used in this study. '*X*' indicates the mole ratio of random incorporation of the ionic comonomer.

used. The mold was set at a temperature of ca. 30 °C. The cooling time was set at 25 s with a hold time of 25 s and a hold pressure of 60 bar.

2.3. Sample preparation

Thin samples were cut from the center of injection-molded tensile specimens. The TEM and X-ray beams were directed through the center of the cross section and parallel to the long axis of the tensile specimen.

2.4. X-ray diffraction

X-ray diffraction (XRD) data were obtained in the transmission mode using a Siemens XPD-700P polymer diffraction system equipped with a two-dimensional, position-sensitive area detector. The sample-to-detector distance was set at 33 cm, which yielded an angular scan from 1.5 to 8° 2θ. The two-dimensional scattering patterns were analyzed using the GADDS™ software package, and the XRD patterns were integrated radially, after background subtraction, to obtain intensity versus scattering angle 2θ plots.

2.5. Transmission electron microscopy

Transmission electron microscopy (TEM) was performed at Eastman Chemical Company. Samples were prepared using a Leica Ultracut UCT microtome with a Diatome ultra diamond knife. Samples were cut from cross-sections of injection molded parts at room temperature approximately 70–100 nm in thickness and collected on EMS 460 Hex Mesh Cu Grids. The cross-sections were lightly coated with carbon using an Edwards Auto 306 carbon coater. A Philips CM12 transmission electron microscope operating at an accelerating voltage of 80 kV and equipped with a Gatan retractable slow scan camera was used to collect images.

2.6. Differential scanning calorimetry

Isothermal crystallization analysis was performed on samples cut from the center portion of injection molded parts using a Perkin–Elmer DSC-7 equipped with an Intracooler 1P. Prior to analysis, the samples were heated to the melt (i.e. 280 °C) for a period of 4 min to normalize the thermal history. The samples were then quenched at the maximum obtainable cooling rate to the isothermal crystallization temperature of 220 °C, and the crystallization exotherm was monitored as a function of time. The half-time of crystallization, $t_{1/2}$, (i.e. the time required for the material to reach 50% of its maximum crystallinity) was used as a quantitative comparison of the rate of bulk isothermal crystallization.

3. Results and discussion

3.1. Morphological characterization of PET/PETI nanocomposites

The spacing between clay platelets, or gallery spacing, is an indicator of the extent of intercalation/exfoliation of clay platelets within a polymer matrix and can be observed by using X-ray diffraction. The scattering curves for the PET based materials containing 5% Cloisite® 10A are shown in Fig. 2. The PET-5% Cloisite® 10A material displays a large peak centered at ca. 2.48° 2θ (ca. 35.6 Å) and a smaller peak located at 5.03° 2θ (17.5 Å). These peaks are attributed to the lamellar arrangement of clay platelets. This distance, corresponding to the d_{001} plane, is termed the gallery spacing of the clay and is dependant on the modification. In contrast, the 'as-received' Cloisite® 10A (in the absence of polymer) has a gallery spacing of 19.2 Å (4.60° 2θ). The

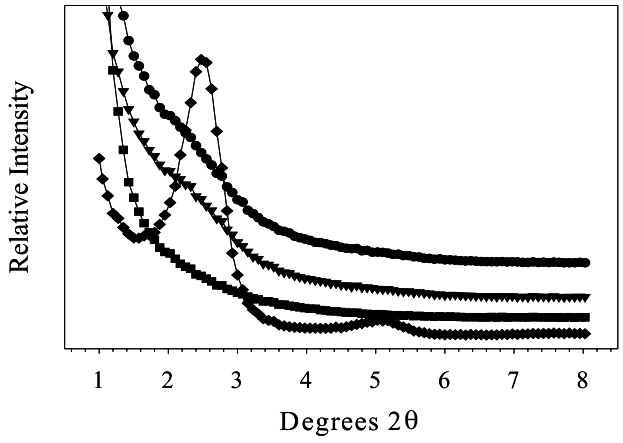

Fig. 2. XRD profiles of the PET and PETI composites containing 5% Cloisite 10A. The PETI systems containing no ionic functionality (♦), 1.8 mol% (■), 3.9 mol% (▼), and 5.8 mol% (●) are offset vertically.

increase in the gallery spacing of the Cloisite® 10A, as observed by XRD, suggests that the clay platelets have been intercalated by the PET. The presence of the higher scattering angle peak in the PET-5% Cloisite® 10A material is attributed to a second order peak from the lower scattering angle peak. The presence of the second order peak suggests that a high degree of periodic order is present in the material. Although the gallery spacing of the clay platelets has been increased through the incorporation of PET, there is still a high degree of layered order present in the clay tactoids.

The XRD of the PET based materials containing 5% Cloisite® 15A are shown in Fig. 3. The PET-5% Cloisite® 15A material displays a peak centered at ca. 2.55° 2θ (ca. 34.6 Å). Alternatively, the 'as-received' Cloisite® 15A has a gallery spacing of 31.5 Å. The slight increase in the gallery spacing of the Cloisite® 15A suggests that very little of the PET intercalated into the gallery space. However, this slight increase in gallery spacing makes it difficult to determine if the Cloisite® 15A is fully intercalated or if a large portion of the clay remained as immiscible aggregates.

In all of the PETI based Cloisite® 10A and Cloisite® 15A materials, shown in Figs. 2 and 3, a decrease in the intensity of the d_{001} peak is observed as the ionic content increases. Furthermore, the second order peak observed in the PET clay sample does not exist in the SAXS data for the PETI nanocomposite. Thus, the presence of the ionic functionality on the PET chain was found to influence the clay platelet dispersion of melt processed samples. The d_{001} peak in the XRD profiles of the PETI(1.8%), PETI(3.9%) and PETI(5.8%) samples containing 5% Cloisite® 15A in Fig. 3 show a decrease in intensity relative to the pure PET sample, and a shift to lower angles (an increase in the gallery size). This peak becomes a weak shoulder in the XRD traces of the nanocomposites containing the ionic species, suggesting that the clay platelets are predominately exfoliated within the ionomer matrices.

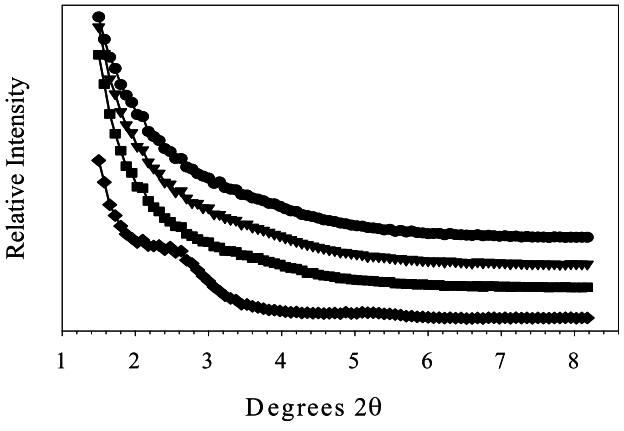

Fig. 3. XRD profiles of the PET and PETI composites containing 5% Cloisite 15A. The PETI systems are offset vertically. The PETI systems containing no ionic functionality (♦), 1.8 mol% (■), 3.9 mol% (▼), and 5.8 mol% (●) are offset vertically.

In order to verify the morphological changes suggested from the XRD observations made above, transmission electron microscopy (TEM) has been used to directly image the samples. Fig. 4 shows a series of TEM micrographs of sectioned injection molded parts of the PET based nanocomposites containing Cloisite® Na. All micrographs have been taken at the same resolution, and the scale bars (0.30 μm) are identical for each sample. In the TEM micrographs, the nanoclay appears as dark areas. The micrograph in Fig. 4(a) is PET containing 5% Cloisite® Na, which shows a tactoid morphology as evidenced by the large groupings of clay platelets appearing as dark regions in the micrograph. These tactoids are areas of clay with little intercalation of the matrix PET chains into the gallery. As ionic functionality is added to the PET backbone, in Fig. 4(b)–(d), the tactoid structure remains relatively unchanged, indicating that the ionic groups on the PETI have little effect on the ability to disperse the Na^+ form clay.

Fig. 5 is a series of TEM micrographs of sectioned injection molded parts of the PET based nanocomposites containing Cloisite® 15A. The micrographs shown have been taken at the same resolution as the TEM micrographs in Fig. 4 for comparison. The micrograph in Fig. 5(a) is PET containing 5% Cloisite® 15A, which shows an intercalated structure at best. Fig. 5(b)–(d) are PETI having 1.8, 3.9, and 5.8% ionic incorporation containing 5% Cloisite® 15A, each of which shows an increasingly more random arrangement of clay platelets in the matrix.

Comparison of the PET based nanocomposites containing either Cloisite® Na, Cloisite® 10A, or Cloisite® 15A are shown in Fig. 6. In Fig. 6(a) the large dark area is indicative the tactoid structure. In Fig. 6(b) and (c), the PET can be seen to somewhat intercalate into the clay galleries. Clearly, the organic modifications to the Cloisite® allow the PET to more easily intercalate the clay galleries. However, even with the shear involved in the extrusion process the pure PET does not appear to significantly exfoliate the clay platelets in the matrix.

Fig. 7 compares the Cloisite® clays when incorporated via melt extrusion into a PETI (1.8%) matrix. As with the pure PET, clay tactoids can still be easily observed when using the Cloisite® Na, shown in Fig. 7(a). However, in contrast to the PET based systems in Fig. 6, when organically modified clays are used, the clay platelets appear more randomly dispersed in the PETI matrix, as seen in Fig. 7(b) and (c), approaching or exhibiting an exfoliated structure. Comparing the two organically modified clays, it appears from the TEM and XRD Cloisite® 10A exfoliates to a greater extent than does Colisite® 15A. These data are in agreement with our previous studies of PBT and PBT-ionomer clay nanocomposites [29]. The enhanced dispersion of clay platelets with increasing ion content for the current PETI systems is somewhat different than what was seen previously in PBTI systems, which showed little dependence of ionic content on dispersion.

From the TEM and XRD data, it can be seen that upon

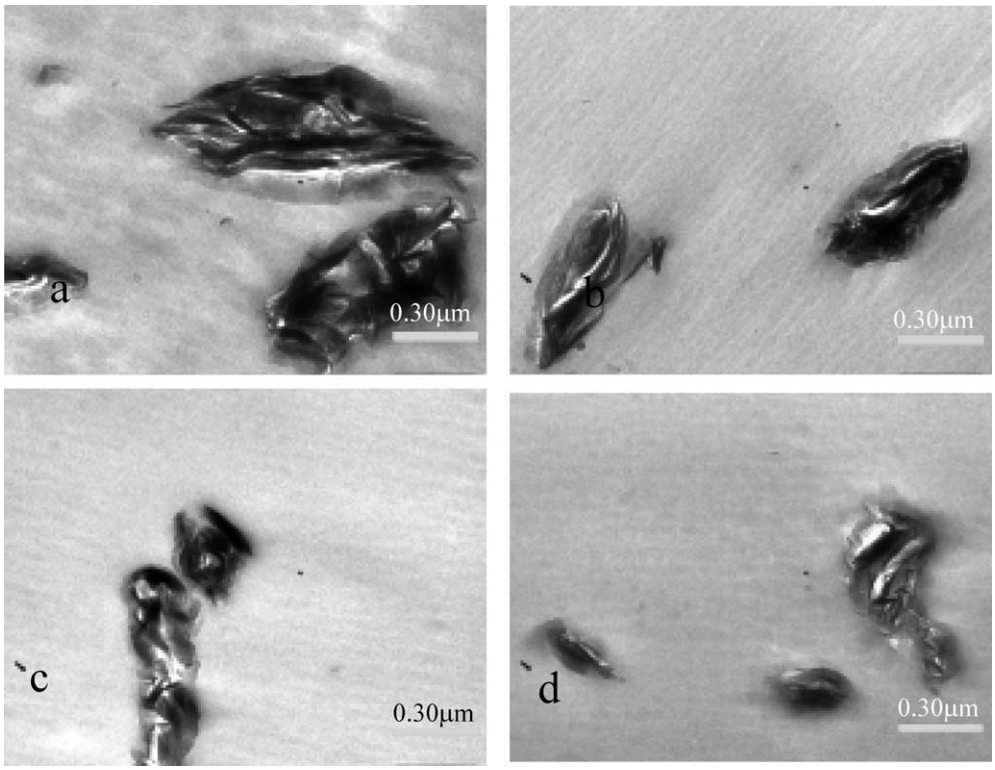

Fig. 4. TEM micrographs of PET (a) and PETI 1.8% (b), 3.9% (c), and 5.8% (d) systems containing 5% Cloisite® Na. The scale bar in all micrographs is 0.30 μm and the magnification is 100,000×.

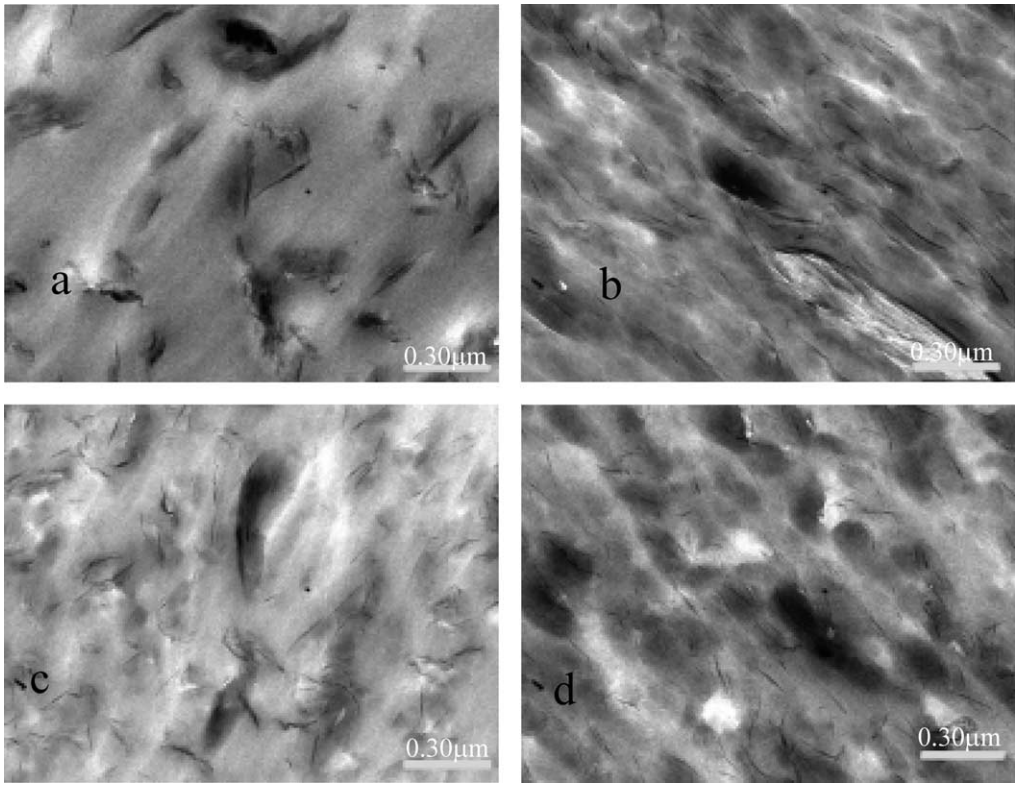

Fig. 5. TEM micrographs of PET (a) and PETI 1.8% (b), 3.9% (c), and 5.8% (d) systems containing 5% Cloisite® 15A. The scale bar in all micrographs is 0.30 μm and the magnification is 100,000×.

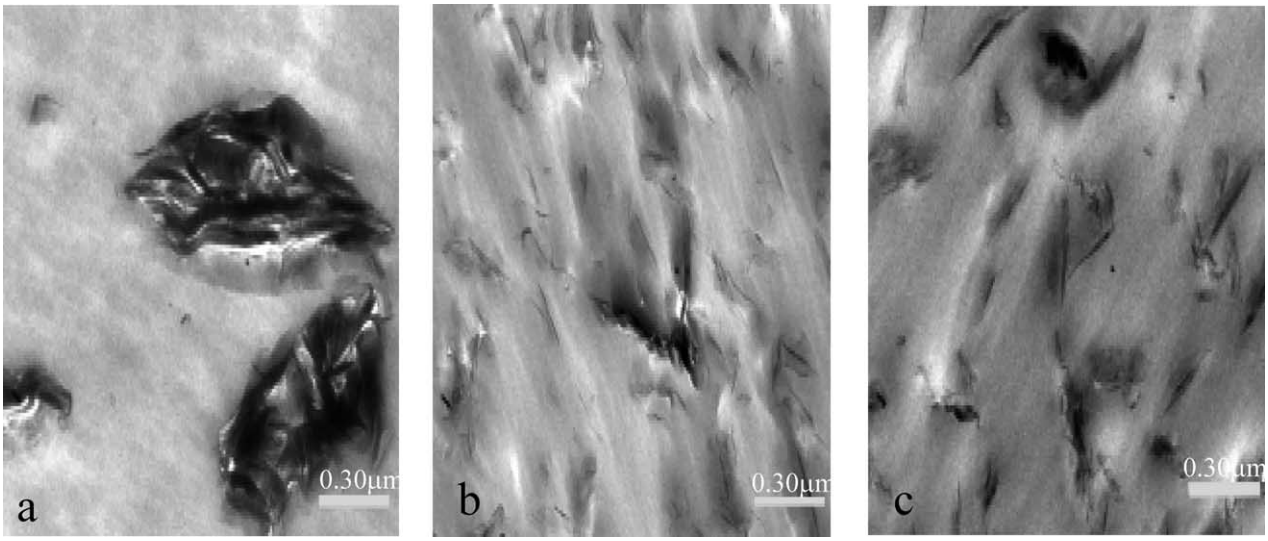

Fig. 6. TEM micrographs of pure PET containing 5% Cloisite® Na (a), 5% Cloisite® 10A (b), and 5% Cloisite® 15A (c).

incorporating the ionic functionality along the PET backbone and organic modification of the clay, the polymer–clay interactions are more favorable leading to better dispersion of clay in the PETI matrix. The reason for these enhanced interactions has been attributed to the ionic interactions between the negatively charged sulfonated groups located randomly along the PET backbone and the positively charged edges of the montmorillonite clay platelets. With these interactions creating an attachment site at the edges of the clay galleries, diffusion of the mobile PET chain segments into the organically modified clay galleries is likely facilitated. This proposed idea is shown schematically in Fig. 8. The diffusion of the mobile PET chain segments into the clay galleries leads to a peeling apart of the clay platelets, resulting in an exfoliated morphology.

3.2. Tensile properties of PET/PETI nanocomposites

The nanoscale morphological differences observed in the XRD and TEM are reflected in the macroscale properties of the nanocomposites. Fig. 9 is a plot of the tensile modulus versus ionic content (expressed as mol% sulfonated groups) for materials containing no clay and materials containing 5 wt% of the OMC. The incorporation of clay into PET increases the tensile modulus from around 1100 MPa for the pure PET to 1500 MPa for the PET nanocomposite containing 5% Cloisite® 10A. As the ionic content is increased, subsequent increases in the tensile modulus can be observed. The substantial improvements in mechanical properties can be attributed to the degree of exfoliation due to the strong interaction between the sulfonic acid groups in

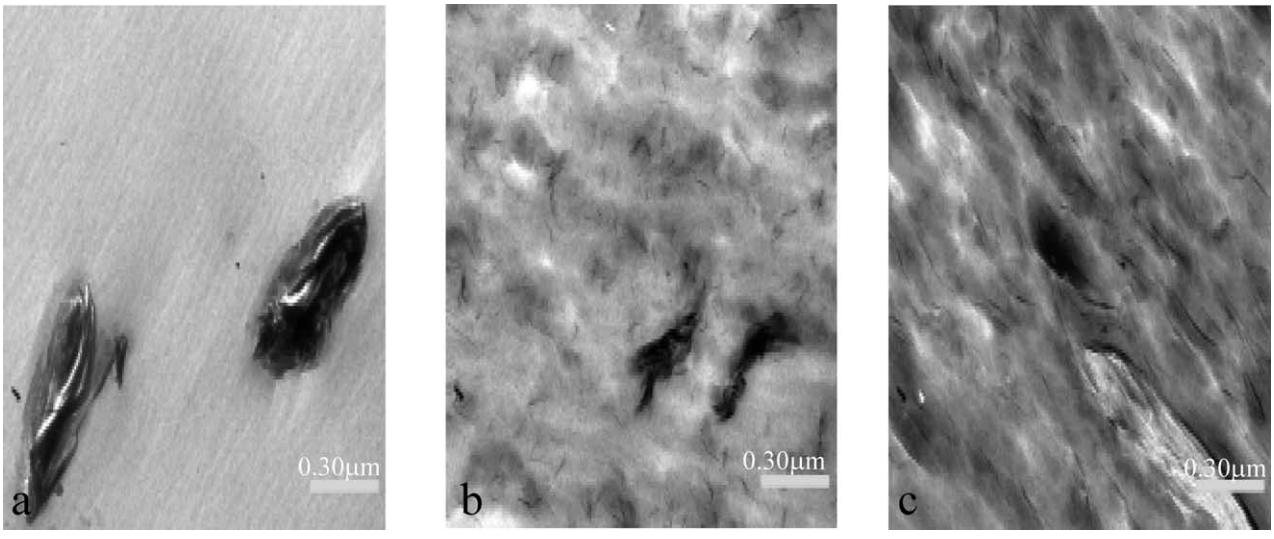

Fig. 7. TEM micrographs of pure PETI 1.8% containing 5% Cloisite® Na (a), 5% Cloisite® 10A (b), and 5% Cloisite® 15A (c).

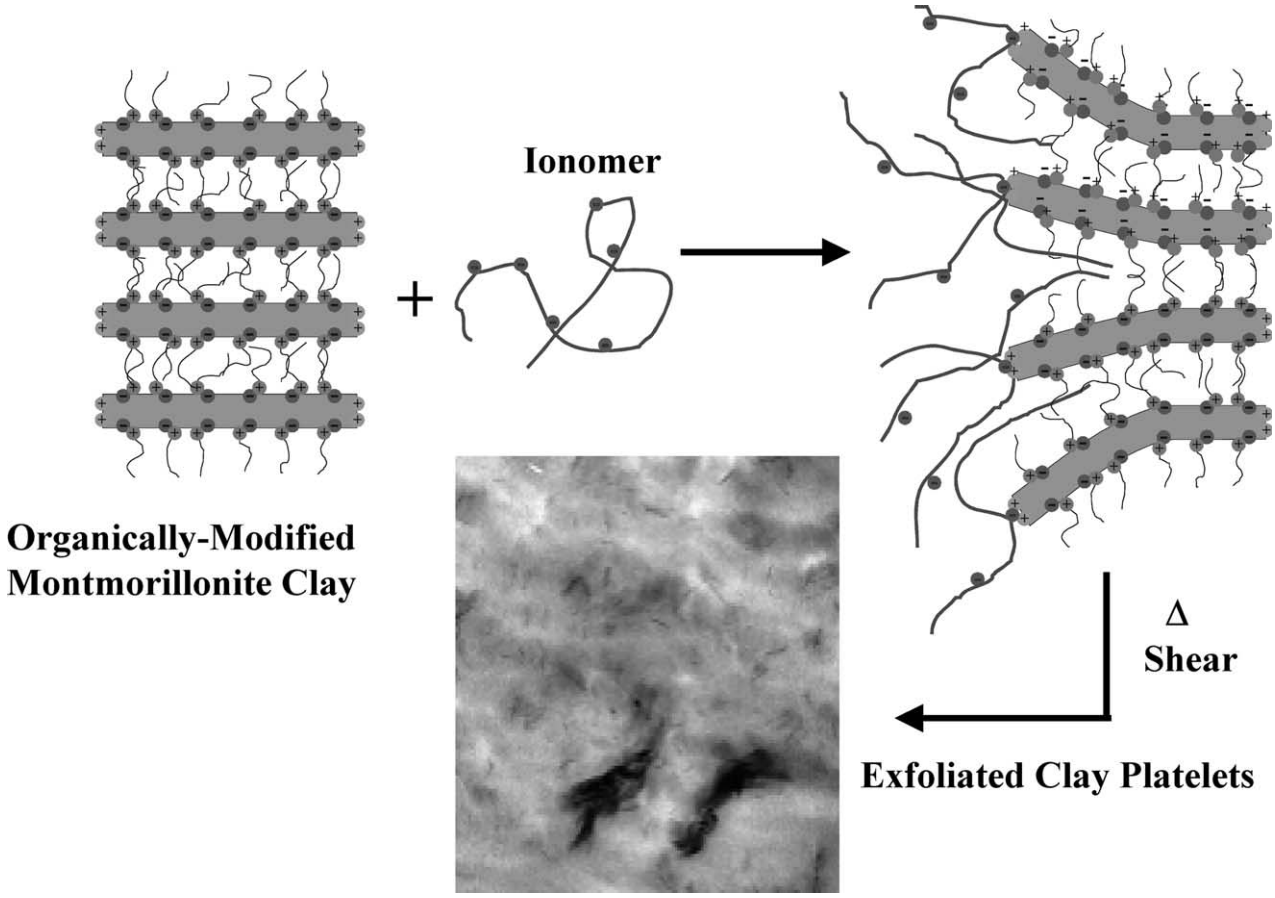

Fig. 8. Schematic representation of the interaction between ionic groups in the polymer backbone and the edges of the clay platelets, leading to a predominately exfoliated morphology.

the PETI matrix and the silicate layers. From these data, Cloisite® 10A appears to be the most favorable organically modified clay for achieving enhanced mechanical properties. In agreement with the morphological behavior (i.e. the best dispersion of platelets is for the PETI/10A systems), this suggests that the organic modification of Cloisite® 10A has more favorable interactions with the PET than does the Cloisite® 15A. The higher tensile modulus samples correspond to those samples that show a more exfoliated type structure via TEM and XRD results.

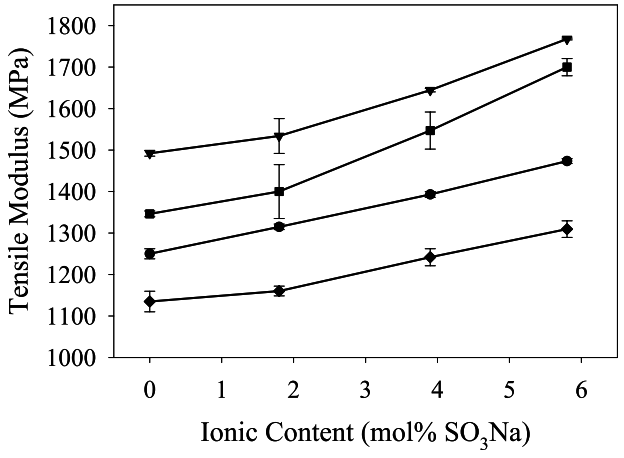

Fig. 9. Plots of tensile modulus vs. clay content for nanocomposites made with PET and PETI. The plot compares the tensile modulus nanocomposites made with no Cloisite® (♦), 5% Cloisite® Na (●), 5% Cloisite® 10A (▼), and 5% Cloisite® 15A (■).

3.3. Crystallization behavior of PET/PETI nanocomposites

The influence of the sodium montmorillonite and organically-modified montmorillonite on the bulk crystallization of the matrix polymers and the respective ionomers was investigated. The half-time of crystallization, $t_{1/2}$, can be used as a quantitative comparison of the rate of bulk isothermal crystallization. Longer crystallization half-times correlate to slower overall rates of bulk crystallization. Table 1 lists the crystallization half-times in minutes for the matrix polymers and the respective 5% clay containing composites. The Cloisite® Na+ containing material had the shortest crystallization half-time of the PET and PETI based composites. The Cloisite® 10A and Cloisite® 15A containing materials had slightly longer crystallization half-times than the PETI matrix. The increased $t_{1/2}$ value of the

Table 1
Isothermal crystallization half-times, $t_{1/2}$, (min), of pure materials and nanocomposites

	Crystallization half-times (min)			
Mol% SO_3Na	0	1.8	3.9	5.8
Pure PET	9.51	3.39	6.17	10.59
Cloisite® Na+	2.11	4.47	5.30	7.61
Cloisite® 10A	2.38	3.59	6.63	12.91
Cloisite® 15A	6.23	4.12	9.04	15.81

organically-modified montmorillonite composites suggests that the presence of the clay influences the PETI matrix crystallization. This observation suggests that Cloisite® 10A and Cloisite® 15A are not as effective as Cloisite® Na+ as a nucleating agent for PET crystallization. While the clay itself may act as a nucleating agent, when the ionic content of the matrix is increased, the crystallization half-time also increase. In the case of the PETI(5.8%), the half-time is greater than that of the PET homopolymer. This increase can be attributed to the increase in the viscosity of the system as the ionic content is increased. Nevertheless, with increased exfoliation (as observed by XRD and TEM) the individual clay particles become less efficient at nucleating PET crystallization, relative to the tactoid state. While the state of intercalation/exfoliation had little effect on the crystallization kinetics in PBTI-clay systems studied previously [29], the phenomenon observed here may be attributed to the presence of interactive surfaces (i.e. the tactoid sides with a periodic arrangement of platelet edges) that are capable of immobilizing chains in conformations that are more favorable for crystallization (i.e. as in epitaxial crystallization). This argument is also consistent with the model shown in Fig. 8.

4. Conclusions

The results of this study show that organic modification of montmorillonite clay coupled with the modification of PET containing low levels (1.8–5.8 mol%) of $-SO_3-Na$ groups results in the production of exfoliated and/or highly intercalated nanocomposites, as evidenced by TEM and XRD, by a simple extrusion process. Low PETI ionic contents, as little as 1.8 mol%, achieved significant exfoliation of the organically-modified montmorillonite clays (Cloisite® 10A and Cloisite® 15A). An identically prepared PET/OMC nanocomposite displays intercalation at best. These results are in complete agreement without previous poly(butylene terephthalate) and poly(butylene terephthalate) ionomer clay nanocomposite studies [29]. It is believed that the ionic interactions created by the incorporation of random sulfonate groups into the backbone of PET aid in the dispersion of the organically modified montmorillonite clay. This has been proposed to occur through electrostatic interactions between the sulfonate groups along the polymer backbone and the edges of the clay platelets, facilitating movement of chain segments attached to the ionic group into the clay gallery. TEM and XRD data also show that an increasing amount of ionic comonomer in the PET backbone increases the apparent degree dispersion of the clay platelets. This behavior is somewhat different than what was seen previously in PBTI systems, which showed little dependence of ionic content on dispersion.

The tensile modulus of the PETI/OMC nanocomposites is greatly improved compared to nanocomposites made from the pure PET. The main reason for the substantial improvements in mechanical properties is the degree of exfoliation due to the strong interaction between the sulfonic acid groups in the PETI matrix and the silicate layers. The higher tensile modulus samples correspond to those samples that show a more exfoliated type structure via TEM and XRD results.

The Cloisite® Na+ clay platelets failed to disperse well within the PET and PETI matrices and remained as large aggregates of clay platelets. Large aggregated clay structures dispersed within polymer matrices result in properties that are similar to microcomposites. However, the organically-modified montmorillonite samples were shown to be exfoliated when dispersed within PETI matrices. The combination of the crystallization data and XRD data suggests that the degree of clay dispersion plays an important role in the polymer crystallization process. The larger aggregates of Cloisite® Na+ were observed to increase the crystallization rate of the polyester ionomers. However, the organically-modified montmorillonite clays, i.e. Cloisite® 10A and Cloisite® 15A, were more dispersed in the polyester ionomer matrices than the Cloisite® Na+. These data suggest that the larger clay aggregates of the Cloisite® Na+ are more efficient in nucleating the polyester matrices than the more finely dispersed Cloisite® 10A and Cloisite® 15A. Moreover, the PETI based Cloisite® 10A and Cloisite® 15A composites had longer crystallization half-times than the matrix polymer or Cloisite® Na+ containing composite. The improved dispersion of the clay platelets may also decrease the crystallization rate of the matrix polymer by increasing the viscosity of the melt.

Acknowledgements

The authors gratefully acknowledge the aid of Dr. Wes Hale and Ken C. Potts at Eastman Chemical, Kingsport, TN, for supplying the PET and PETI samples and for performing the TEM analysis, respectively. Financial support of this program was provided through the MS NSF EPSCoR program and Eastman Chemical.

References

[1] Ibbotson C, Sheldon RP. Br Polym J 1979;11:146.

[2] Legras R, Bailly C, Daumerie M, Dekoninck JM, Mercier JP, Zichy V, et al. Polymer 1984;25:835.
[3] Legras R, Dekoninck JM, Vanzieleghem A, Mercier JP, Nield E. Polymer 1986;27:109.
[4] Wang X, Zhu Z, Bu H. Acta Polym 1995;46:163.
[5] Matayabas JC, Turner SR. In: Pinnavaia TJ, Beall GW, editors. Polymer–clay nanocomposites. Chichester: Wiley; 2000. p. 207–25.
[6] Sekelik DJ, Stepanov EV, Nazarenko S, Schiraldi D, Hiltner A, Baer E. J Polym Sci, Part B: Polym Phys 1999;37:847.
[7] Giannelis EP. Adv Mater 1996;8:29.
[8] Legaly G. Appl Clay Sci 1999;15:1.
[9] Chang J-H, Kim SJ, Joo YL, Im S. Polymer 2004;45:919.
[10] Liu W, Tian X, Cui P, Li Y, Zheng K, Yeng Y. J Appl Polym Sci 2004;91:1229.
[11] DiLorenzo ML, Errico ME, Avella M. J Mater Sci 2002;37:2351.
[12] Lee S-S, Kim J. Polym Sci Eng 2003;89:370.
[13] Ke Y, Long C, Qi Z. J Appl Polym Sci 1999;71:1139–46.
[14] Ke Y-C, Yang Z-B, Zhu C-F. J Appl Polym Sci 2002;85:2677–91.
[15] Imai Y, Nishimura S, Abe E, Tateyama H, Abiko A, Yamaguchi A, et al. Chem Mater 2002;14:477.
[16] Saujanya C, Imai Y, Tateyama H. Polym Bull 2002;49:69.
[17] Saujanya C, Imai Y, Tateyama H. Polym Bull 2003;51:85.
[18] Imai Y, Inukai Y, Tateyama H. Polym J 2003;35:230.
[19] Sanchez-Solis A, Garcia-Rejon A, Manero O. Macromol Symp 2003; 192:281.
[20] Davis CH, Mathias LJ, Gilman JW, Schiraldi DA, Shields JR, Trulove P, et al. J Polym Sci, Part B: Polym Phys 2002;40:2661.
[21] Pegoretti A, Kolarik J, Peroni C, Migliaresi C. Polymer 2004;45:2751.
[22] Wang Y, Shen C, Chen J. Polym J 2003;35:884.
[23] Wang Y, Shen C, Li H, Li Q, Chen J. J Appl Polym Sci 2004;91:308.
[24] Ou CF, Ho MT, Lin JR. J Polym Res 2003;10:127.
[25] Ou CF, Ho MT, Lin JR. J Appl Polym Sci 2004;91:150.
[26] Barber GD, Carter CM, Moore RB. ANTEC 2000;3:3763.
[27] Carter CM. ANTEC 2001;3:3210.
[28] Ostrowska-Gumkowska B. Eur Polym J 1994;30:875–9.
[29] Chisholm BJ, Moore RB, Barber G, Khouri F, Hempstead A, Larsen M, et al. Macromolecules 2002;35:5508.